Journal of Biomedical Optics

SPIEDigitalLibrary.org/jbo

Cyanine dyes as contrast agents for near-infrared imaging *in vivo*: acute tolerance, pharmacokinetics, and fluorescence imaging

Bernd Ebert
Björn Riefke
Uwe Sukowski
Kai Licha

SPIE

Cyanine dyes as contrast agents for near-infrared imaging *in vivo*: acute tolerance, pharmacokinetics, and fluorescence imaging

Bernd Ebert,[a] Björn Riefke,[b] Uwe Sukowski,[a,*] and Kai Licha[c]
[a]Physikalisch-Technische Bundesanstalt, Abbestr. 2-12, Berlin, 10587 Germany
[b]Bayer Healthcare, Laboratory Diagnostics Non-Clinical Drug Safety, Berlin, Germany
[c]mivenion GmbH, Berlin, Germany

Abstract. We compare pharmacokinetic, tolerance, and imaging properties of two near-IR contrast agents, indocyanine green (ICG) and 1,1′-bis-(4-sulfobutyl) indotricarbocyanine-5,5′-dicarboxylic acid diglucamide monosodium salt (SIDAG). ICG is a clinically approved imaging agent, and its derivative SIDAG is a more hydrophilic counterpart that has recently shown promising imaging properties in preclinical studies. The rather lipophilic ICG has a very short plasma half-life, thus limiting the time available to image body regions during its vascular circulation (e.g., the breast in optical mammography where scanning over several minutes is required). In order to change the physicochemical properties of the indotricarbocyanine dye backbone, several derivatives were synthesized with increasing hydrophilicity. The most hydrophilic dye SIDAG is selected for further biological characterization. The acute tolerance of SIDAG in mice is increased up to 60-fold compared to ICG. Contrary to ICG, the pharmacokinetic properties of SIDAG are shifted toward renal elimination, caused by the high hydrophilicity of the molecule. N-Nitrosomethylurea (NMU)-induced rat breast carcinomas are clearly demarcated, both immediately and 24 h after intravenous administration of SIDAG, whereas ICG shows a weak tumor contrast under the same conditions. Our findings demonstrate that SIDAG is a high potential contrast agent for optical imaging, which could increase the sensitivity for detection of inflamed regions and tumors. [DOI: 10.1117/1.3585678]

Keywords: cyanine dyes; contrast agents; fluorescence imaging; breast cancer; inflammation.

Paper 11055R received Feb. 4, 2010; revised manuscript received Mar. 30, 2011; accepted for publication Apr. 8, 2011; published online Jun. 14, 2011.

1 Introduction

Laser-induced fluorescence imaging is a nonionizing, harmless, and highly sensitive diagnostic procedure that is emerging in many different medical fields as a noninvasive technique for disease imaging and tissue characterization. Important applications for fluorescence imaging and fluorescent dyes as contrast agents are the recently developed methods for detection of rheumatoid arthritis,[1] optical mammography,[2] and intraoperative imaging in surgery[3] in which reasonable improvements in equipment technology and image algorithms for analysis have been achieved during the last several years. For planar and tomographical optical imaging of the breast, wavelengths in the range between 700 and 900 nm are used for deeper tissue penetration of diffusing photons up to several centimeters.[4] In this optical window of tissue, the absorption by the major intrinsic chromophores hemoglobin and water shows lowest values.[4] Indocyanine green (ICG) is meanwhile established as imaging agent in ophthalmology, surgery, and inflammation imaging,[1–3,5,6] but remains without a reasonable clinical follow-up candidate until today.

The potential of fluorescent conjugates with antibodies,[7,8] small peptides,[9] and macromolecules[10] or enzymatically activatable fluorescent probes[11] was demonstrated in numerous studies using sensitive fluorescence imaging techniques in experimental tumor models. However, beside the known disadvantages of possible allergic reactions, tumor physiology and changed receptor or enzyme status during tumor development,[12,13] these probes are of a rather complicated chemical blueprint, making it difficult and expensive to thoroughly assess the toxicological profile of both parent compound, as well as metabolites and degradation products.

Accordingly, the application of hydrophilic low molecular weight compounds of high tolerability, as used in computer tomography (CT) and magnetic resonance imaging (MRI) imaging, might offer a feasible alternative. Iodinated contrast media showed a good potential in the differentiation between benign and malignant breast lesions in clinical trials with CT.[14,15] Dynamic gadolinium-diethylenetriamine penta-acetic acid (Gd-DTPA) enhancement in tumors has been successfully used in nonionizing MRI mammography as valuable and reliable parameter for breast lesion differentiation.[16,17] The amount of early tumor enhancement is used to increase the sensitivity, whereas the temporal pattern of contrast media enhancement can be used to increase the specificity of the method.[18] A rapid and pronounced enhancement within the first 1–2 min followed by a faster washout of Gd-DTPA compared to normal tissue are considered to be an indicator for malignancy. A weaker and sustained enhancement over time is possibly an indicator for inflammatory disease.[19]

*Present affiliation: Bundesministerium für Wirtschaft und Technologie, Berlin, Germany.

Address all correspondence to: Bernd Ebert, Biomedical Optics, Physikalisch-Technische Bundesanstalt, Abbestrasse 2-12, Berlin, 10587 Germany; Tel: 49-30-3481-7384; Fax: 49-30-3481-7505; E-mail: bernd.ebert@ptb.de.

1083-3668/2011/16(6)/066003/9/$25.00 © 2011 SPIE

It is obvious to consider the pharmacological profile of the low molecular weight dye ICG in the light of other small contrast agents. However, ICG has properties different from agents, such as Gd-DTPA. It is strongly bound to plasma proteins, shows negligible extravasation, and is rapidly taken up by the liver.[20–22] Therefore, plasma levels are falling within minutes after intravenous (i.v.) administration to low values.

In order to alter the pharmacokinetic behavior of ICG for a possible improvement in imaging applications, we adapted the physicochemical properties from known x-ray and MRI contrast agents[23,24] for the design toward biological inert hydrophilic low-molecular-weight cyanine dyes. For the dye 1,1′-bis-(4-sulfobutyl) indotricarbocyanine-5,5′-dicarboxylic acid diglucamide monosodium salt (SIDAG), this could be achieved similarly to x-ray agents by decorating the structure with hydrophilic polyhydroxy residues, thereby leading to the first sugar-derivatized cyanine dye described.[25–27] Although the physically effective chemical cyanine entity is of a completely different chemical structure when compared to a paramagnetic DTPA complex moiety or a triiodinated aromatic x-ray absorber, the exterior structural modifications with hydroxyl groups and anionic charge are similar, thus attributing comparable physicochemical properties to the entire molecule. These are a low partition coefficient and low plasma protein binding, which is expected to translate *in vivo* into an increase in tolerability[28] while exhibiting an altered contrasting profile.[29]

The objective of this study was to investigate the acute tolerance of the dye SIDAG compared to ICG in mice and to elucidate the pharmacokinetic and elimination characteristics of both dyes in a rat model. Additionally, we evaluated the ability of both dyes, how to improve contrast in reflection images for *in vivo* tumor visualization using a sensitive fluorescence imaging device.

2 Materials and Methods

2.1 *Cyanine Dyes*

The indotricarbocyanine dye SIDAG was synthesized and prepared as a lyophilized powder with a purity of 98% as described earlier.[25] For *in vivo* experiments lyophilized dye SIDAG was dissolved in sterile 0.9% sodium chloride (Braun Melsungen, Germany). The reference substance ICG was purchased as ICG-Pulsion® from Pulsion Medical Systems (Munich, Germany). Test solutions of dyes were prepared directly prior to use. The chemical structures are shown in Fig. 1. The dye concentration in solution was adjusted by determination of sulfur content using an ion-coupled-plasma-absorption-emission spectroscope (ICP-AES ARL 3560 B ICP Analyzer, Nicolet ARL, Offenbach, Germany).

2.2 *Acute Tolerance*

Acute tolerance was tested after single intravenous injection in male Naval Medical Research Institute mice (Bayer Schering Pharma AG) of 18–22 g weight. ICG served as reference. The contrast media were injected at various doses into a tail vein of up to two animals per dose. The behavior of the animals and the lethality was monitored for seven days post-injection (p.i.).

2.3 *Pharmacokinetics*

The plasma levels and elimination characteristics of SIDAG and ICG were compared using three Han-Wistar rats of 200 g

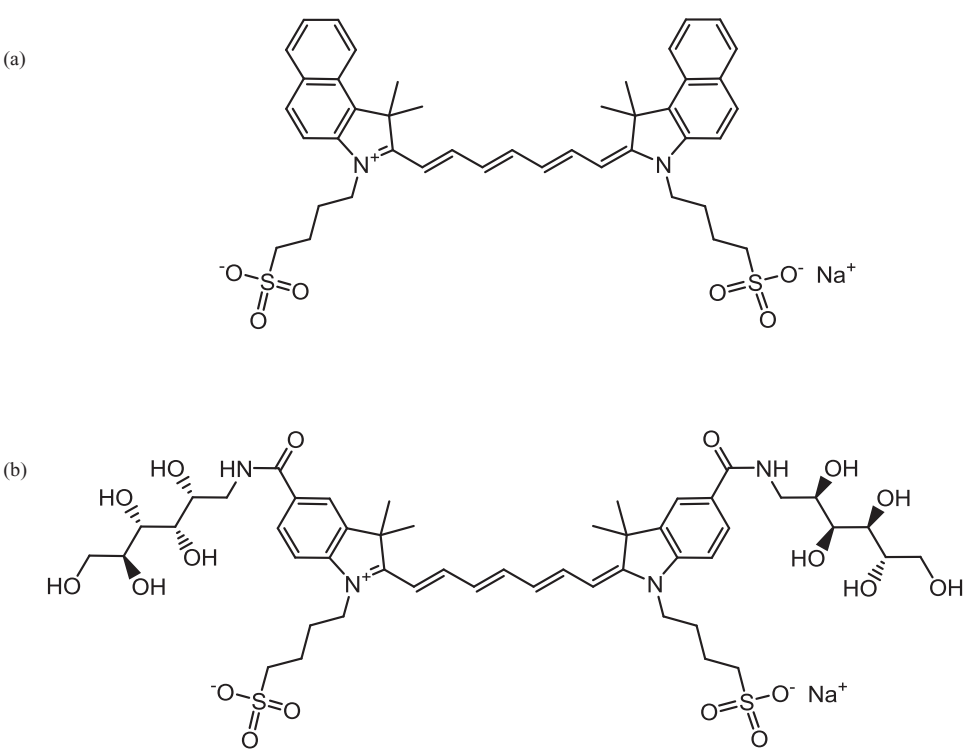

Fig. 1 Chemical structures of investigated low molecular weight cyanine dyes. (a) ICG (MW: 775 g mol^{-1}), (b) SIDAG (MW: 1089.2 g mol^{-1}).

weight per substance. For surgical preparation of catheters, rats were anaesthetized with 250 μL Tilest® 100 (Parke Davis, Freiburg, Germany) and 30 μL Rompun®, 2% solution, (Bayer, Leverkusen, Germany) intra-muscular (i.m.). During the experiment, anesthesia was controlled by reflex control and maintained with 50 μL Tilest. Dyes were administered intravenously via a polyethylene catheter in the *V. jugularis* at a dose of 2.18 mg kg^{-1} (SIDAG) or 1.55 mg kg^{-1} (ICG), equivalent to a dose of 2 μmol kg^{-1} for both dyes. Via a polyethylene catheter, samples were taken at different time intervals after intravenous dye administration from blood, bile, and urine of the same animal. Control samples of blood, bile, and urine were taken prior to dye injection as solvents for calibration measurements to determine absorption coefficients in the respective media. Blood samples with a total volume of 700 μl were collected at 2, 5, 15, 30, 60, 90, 120, and 240 min p.i. via the *A. carotis*.

Blood samples containing a mixture of 400 μl blood and 300 μl 0.9% NaCl/Liquemin were centrifuged for 10 min at 3500 rpm. (Biofuge A, Hereaus, Hanau, Germany). The resulting supernatants, and plasma samples were stored at –70°C for further measurements. Samples of bile and urine were collected via catheters in the ductus choledochus and bladder at 15, 30, 60, 90, 120, 150, and 240 min after dye administration and stored at –70°C for further measurements. During the experiments, the body temperature of anaesthetized animals was kept constant at 38°C using a heating pad.

The dye concentrations in plasma, bile, and urine samples were determined photometrically using a Lambda 2 spectrophotometer (Perkin Elmer, Überlingen, Germany). Prior to measurements, plasma samples were incubated for 1 h at 55°C in a water bath. Denatured proteins were removed by centrifugation for 60 min at 13 $\times$ 10^3 rpm in an Eppendorf centrifuge. An aliquot of the plasma sample was diluted with water, and an absorption spectrum was measured against water as a reference. Samples of bile and urine were centrifuged for 15 min at 13 $\times$ 10^3 rpm and diluted with water. Spectroscopic measurements were performed as described earlier. Dye concentrations were calculated using the extinction coefficients in the corresponding media, which were determined separately for each experiment. The following pharmacokinetic parameters were calculated using the software package TOPFIT (version 2.1ß, Thomae GmbH, Gödecke AG, Schering AG, Germany) plasma half-life in the distribution phase ($t_{(1/2)\alpha}$), terminal half-life ($t_{(1/2)\beta}$), volume of distribution (V_c), the volume in steady-state(V_{ss}), the blood clearance (clearance), and the estimated concentration at time 0 (C_0).

2.4 *Tumor-Bearing Animals*

Mammary tumors were chemically induced in six female rats at an age of 55 $\pm$ 3 days by single intravenous administration of NMU (Sigma, Germany) dissolved in physiological saline at a dose of 50 mg/kg. Injection volume was adjusted to 1.5 ml per 200-g rat. Tumors developed within six to eight weeks after chemical induction at one or multiple sites at the milk ducts of the animals. To reduce autofluorescence in the animals caused by normal food, animals were fed with a Mn-free diet for 10–14 days prior experiments. For imaging experiments, both lateral and ventral part of the rat bodies were shaved uniformly in order to compare tumor fluorescence to the surrounding normal tissue.

All animal experiments have been approved by the Senator für Gesundheit und Soziales, Berlin, Germany. Care and management of the animals were in compliance with the European Community guidelines.

2.5 *Fluorescence Imaging*

An experimental setup adapted from Ref. 27 was used for *in vivo* fluorescence imaging of tumor bearing animals and is shown in Fig. 2. An optical parametric oscillator (OPO, GWU-Lasertechnik, Erftstadt, Germany) with β-BaB_2O_4 as the nonlinear medium, pumped by the third harmonic (λ = 355 nm, E_{pulse} = 100 mJ) of a Q-switched Nd:YAG laser (GCR-230, Spectra-Physics Inc., Darmstadt, Germany), provided laser radiation tunable between 410 nm and 2.2 μm. The energy and the duration of the output pulses at λ = 740 nm amounted typically to 1 mJ and 3 ns. The laser beam was coupled into a 600-μm hard clad silica fiber. The fiber was scrambled, and the output side was kept nearby the objective at a distance that provided an illuminated area of ~200 mm diam. Two long-pass filters were used ($\lambda_{50\%}$ = 750 nm, $\lambda_{50\%}$ = 800 nm) to cut off scattered excitation light. The fluorescence was imaged using a cooled, intensified charge-coupled device (CCD) camera (Model ICCD-576, Princeton Instruments Inc., Trenton, New Jersey) equipped with a standard lens of 50 mm focal length. In order to record fluorescence images synchronized to the laser pulse, the intensifier of the CCD camera was gated by an electrical pulse (–80 V) of ~20-ns duration derived from a high-voltage (HV) pulse generator. The HV pulse generator was triggered by a pulse provided by the power supply of the Nd:YAG laser and appropriately delayed by means of a digital delay generator. Because of the small fluorescence decay time of cyanine dyes (~300 ps) compared to tissue autofluorescence (~3 ns) prompt fluorescence images have been detected. The aperture and exposure time were varied to determine the fluorescence intensities in tumors and normal tissues at different time intervals after administration.

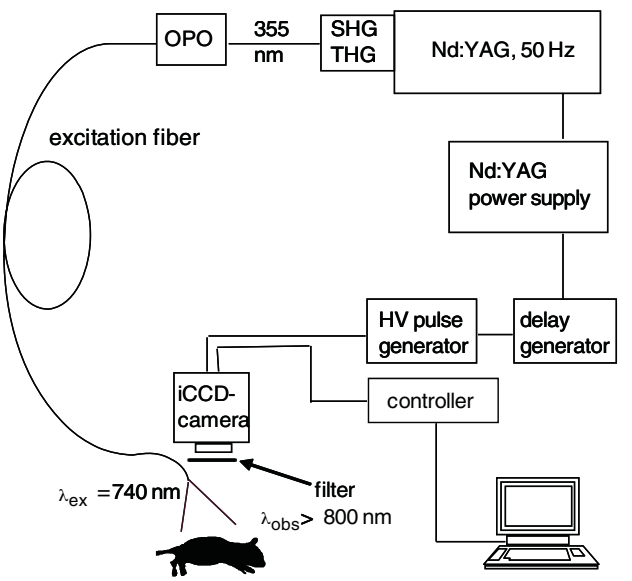

Fig. 2 Experimental setup for *in vivo* fluorescence imaging experiments.

Fluorescence images were taken before, as well as 1 min, 10 min, 60 min, and 24 h after intravenous dye administration via a lateral tail vein at a standard dose of 2.18 mg kg^{-1} (SIDAG) or 1.55 mg kg^{-1} (ICG). Animals were anesthetized with 250 μl of a mixture containing 8.33 parts Tilest 100 and 1 part Rompun i.m. During the experiment, anesthesia was controlled by reflex control and maintained with 100 μl Tilest/Rompun i.m. when necessary. Throughout the experiments, the body temperature of the animals was kept constant at 38°C with a heating pad.

2.6 *Data Processing and Image Analysis*

Fluorescence images were stored and analyzed using the WinView™ software (Princetown Instruments Inc., Trenton, New Jersey). In order to calculate tumor-to-tissue contrast, the fluorescence intensities of tumor and surrounding normal tissue were determined using statistic functions of the WinView software. The resulting mean fluorescence intensities were corrected for aperture and exposure time. The fluorescence intensities of tumor tissue were normalized to intensities taken from contralateral regions, if possible, or from surrounding normal tissue.

3 Results

3.1 *Acute Tolerance*

The results of acute tolerance and of approximate LD_{50} are summarized in Table 1. For ICG, the acute tolerance in mice was estimated to be in the range of 62 mg kg^{-1}. On the contrary, the hydrophilic dye SIDAG possesses a much higher acute tolerance. No toxic reaction of the animals could be observed up to a dose of 5446 mg kg^{-1}, the highest dose tested. Thus, the approximate LD_{50} is estimated to be >5446 mg kg^{-1}.

3.2 *Pharmacokinetics*

Plasma levels and elimination characteristics of SIDAG were studied in a rat model in comparison to ICG. Plasma levels of the reference compound ICG were decreasing immediately after dye administration (Fig. 3). An ICG concentration of 0.62 ± 0.2 3 mg ml^{-1} ICG, corresponding to 1.3 ± 0.5% of the injected dose, was measured 30 min after dye administration.

Table 1 Acute tolerance ($LD_{50\ approx}$) of SIDAG and ICG after single intravenous administration in mice. Number of dead animals/number of tested animals (n_d/n).

	ICG		SIDAG	
Substance	Dose (mg kg^{-1})	(n_d/n)	Dose (mg kg^{-1})	(n_d/n)
	70	2/2	5446	0/2
	62	1/2	3268	0/1
	54	0/2	1634	0/1
			1089	0/1
$LD_{50\ approximate}$ (mg kg^{-1})	62		>5446	

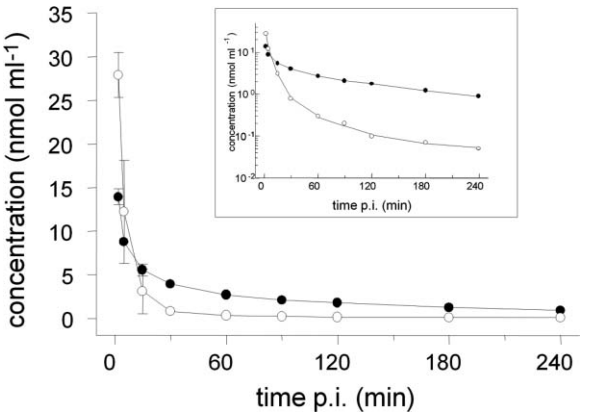

Fig. 3 Time course of plasma concentrations of SIDAG and ICG after intravenous injection in rats. Dose: 2.12 mg kg^{-1} (M ± SD; $n = 3$) SIDAG and 1.55 mg kg^{-1} ICG. These doses are equivalent to a dose of 2 μmol kg^{-1} for both dyes, which is used for comparability in this presentation. Key: (●) SIDAG, (○) ICG. Inset: Plasma distribution of SIDAG and ICG with logarithmic scale.

The half-life time of elimination of ICG was determined to be 25 ± 17 min. The distribution of ICG in the vascular space was indicated by V_c with 64.4 ± 7.2 ml/kg (Table 2). ICG was eliminated via the hepatobiliary pathway, with 82 ± 5% of the injected doses being found in the bile 4 h p.a. No ICG was found in the urine of the animals (Fig. 4).

Plasma levels for SIDAG found after the distribution phase of SIDAG were 4.36 ± 0.33 mg ml^{-1}, corresponding to 6.4 ± 0.4% of the injected dose at 30 min p.a. (Fig. 3). The half-life time of plasma elimination of SIDAG is 89 ± 15 min, thus 3.6 times longer compared to ICG. Plasma levels fall biexponentially to lower levels (Fig. 3, inset). The volume of distribution of SIDAG is in the range of extracellular water with a

Table 2 Pharmacokinetic parameters of low molecular weight cyanine dye SIDAG and ICG after intravenous administration in rats.

Plasma distribution	ICG	SIDAG
$t_{1/2\alpha}$(min)	1.8 ± 0.1	3.7 ± 1.3
$t_{1/2\beta}$(min)	25 ± 17	89 ± 15
V_C(ml kg^{-1})	64.0 ± 7.2	137 ± 8.4
V_{SS}*(ml kg^{-1})	233 ± 162	365.0 ± 11.1
Clearance(ml min^{-1} kg^{-1})	12.0 ± 4.5	3.2 ± 0.7
C(0)(nmol ml^{-1})	31.0 ± 3.4	15 ± 0.9
Hepatobiliary elimination		
A_{bile}(% I.D)	82 ± 5	0.8 ± 0.4
Renal elimination		
A_{urine}(% I.D.)	–	68 ± 10

*Steady state concentration of dye in plasma.

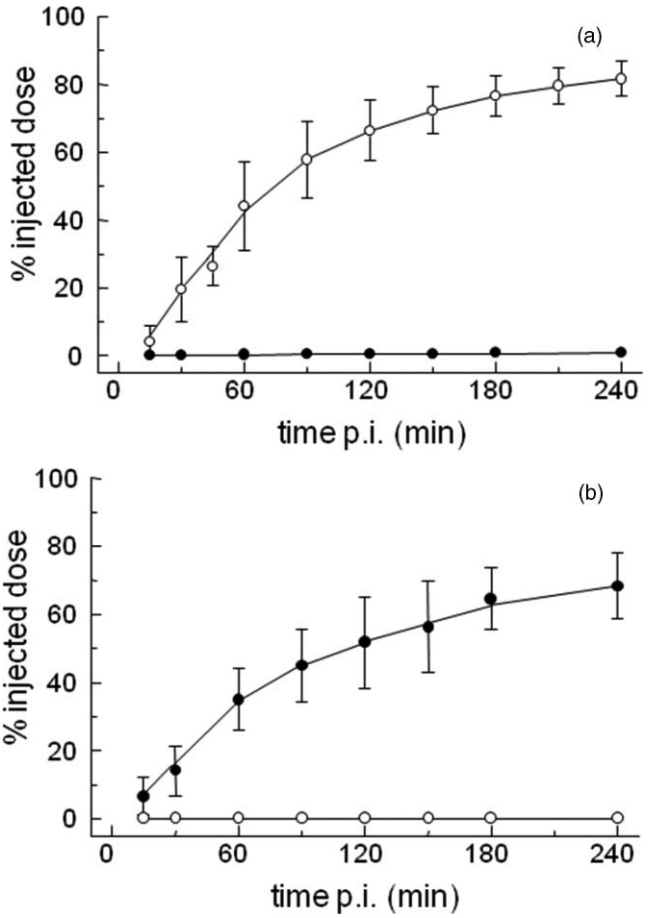

Fig. 4 Time course of SIDAG and ICG in (a) bile and (b) urine after i.v. injection of contrast media in three rats per dye (M ± SD; $n = 3$). Dose: 2.12 mg kg^{-1} SIDAG and 1.55 mg kg^{-1} ICG. Key: (●) SIDAG, (○) ICG.

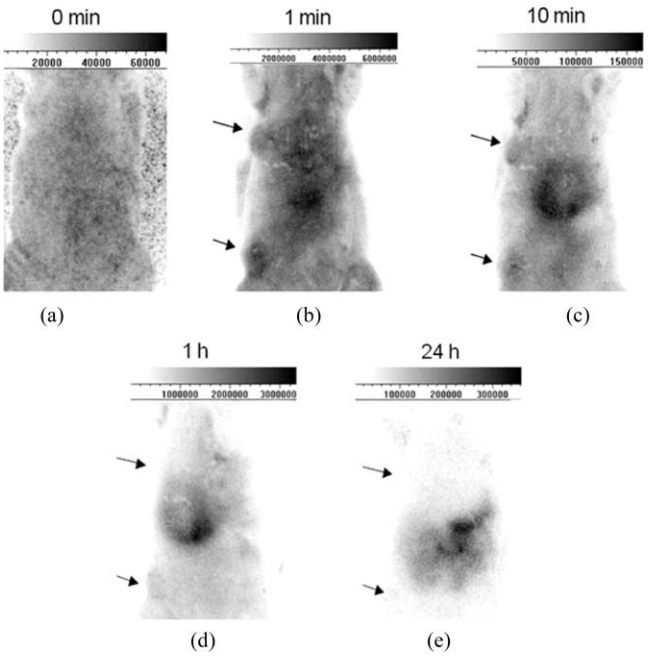

Fig. 5 Fluorescence images of tumor bearing rat (NMU-induced rat breast carcinoma) using indocyanine green at a dose of 1.55 mg kg^{-1}. (a) anterior view before i.v. dye injection, (b) anterior view 1 min p.a., (c) anterior view 10 min p.a., (d) anterior view 60 min p.a., and (e) anterior view 24 h p.i. Arrows indicate tumor localization.

value of $V_c = 137 \pm 11.1$ ml/kg (Table 2). The main part (68 ± 10%) of the injected dose measured at 4 h p.i. in the urine of the hydrophilic cyanine dye SIDAG is predominantly excreted via the renal pathway. Only negligible amounts of 0.8 ± 0.4% of the injected dose of SIDAG were found in the bile after dye administration (Table 2 and Fig. 4).

3.3 *Fluorescence Imaging*

The fluorescence imaging properties of SIDAG were evaluated in comparison to ICG in six animals with NMU-induced breast tumor-bearing rats, three for each dye. The autofluorescence background of tissue before injection of contrast media in the near-infrared region is generally low. Tumors could not be distinguished clearly from surrounding tissue before dye administration in the fluorescence images. The intensity of fluorescence background of tumor tissue was slightly lower than that of normal tissue. The fluorescence ratio of tumor region to the contralateral region of the animal for the groups investigated with SIDAG and with ICG was determined to 0.86 ± 0.10 and 0.93 ± 0.10, respectively. A typical sequence of fluorescence images after ICG administration is shown in Fig. 5. A 125-fold increase in average fluorescence intensity was observed 1 min postinjection of ICG in tumor tissue and 113-fold increase in normal tissue compared to autofluorescence background. A decrease of fluorescence intensity both in tumor tissue and normal tissue was found at 10 min p.i., followed by a further decrease toward baseline levels at 1 and 24 h. At 24 h p.i., fluorescence intensity of normal tissue has reached nearly background levels. Already at 1 min after ICG administration, the highest fluorescence intensities were found in the liver region of the animals followed by a further increase in this region at 10 min and 1 h p.i. At 24 h, the highest fluorescence intensities were found in the liver region and in the gastrointestinal tract of the animals. NMU-induced breast tumors could only marginally be demarcated from surrounding normal tissue after injection of ICG, shown quantitatively by tumor-to-normal tissue ratio of 1.13 ± 0.07 at 1 min p.i. (Fig. 6).

A typical sequence of fluorescence images using SIDAG is shown in Fig. 7. The increase of fluorescence intensity 1 min p.i. of SIDAG was about 197-fold for tumors, whereas in normal tissues a 126-fold increase was observed [Fig. 8(a)]. The fluorescence intensity in both tumor and normal tissue reached the maximum at 10 min p.i. and decreased subsequently as indicated by lower absolute values at 1 h and 24 h p.i. At 24 h p.i., fluorescence levels were slightly higher than baseline levels for ICG and clearly higher for SIDAG, as shown in Fig. 8(b). With the use of SIDAG, tumors could be clearly separated from surrounding normal tissue 1 min p.i. with intensity ratios between tumors and normal tissue of 1.33 ± 0.14. Tumors of multiple size and at different locations could be detected as shown in Fig. 7. With ongoing time, tumor contrast decreased slightly at 10 min. Again at 24 h p.i., a high ratio between tumors and normal tissue of 2.78 ± 0.17 was observed with clear tumor delineation (Fig. 7).

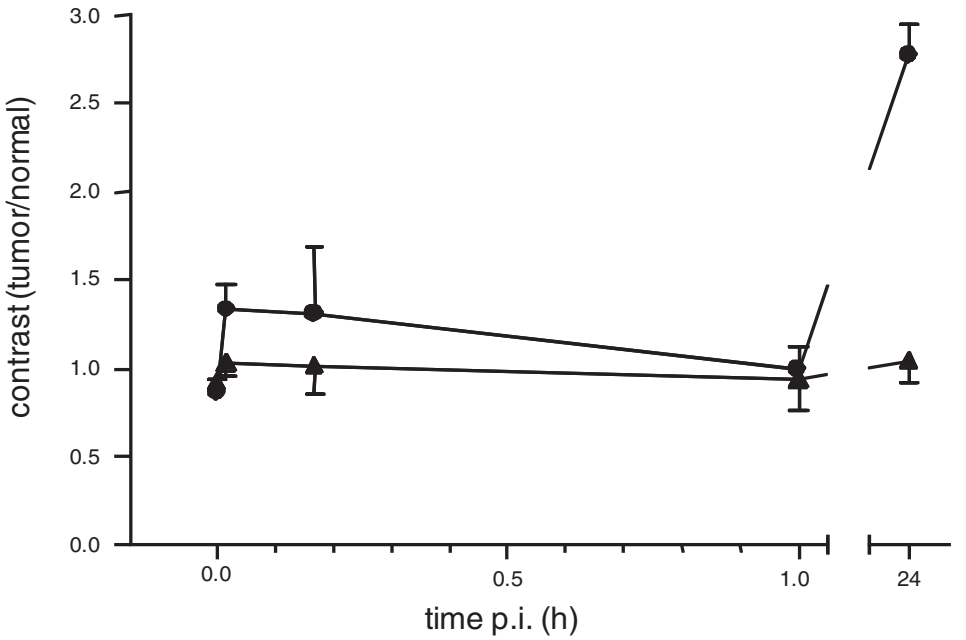

Fig. 6 Tumor-to-normal tissue contrast after i.v. administration of SIDAG (●) and ICG (▲) in NMU-induced rat breast tumors bearing rats at different times of dye administration and a dose of 2.12 mg kg^{-1} (SIDAG) and 1.6 mg kg^{-1} (ICG).

4 Discussion

The application of contrast agents for diffuse optical imaging may contribute to improve the diagnostic potential of this non-invasive method. The dye ICG is clinically approved for microvascular imaging and angiography, and currently finds increased application in surgery[3] and lymphatic imaging using optical techniques.[30] The fast plasma clearance caused by rapid liver uptake challenges imaging performance, which requires fast systems capable of monitoring the rapidly changing concentration of the dye after administration. Higher contrast may be obtained if concentrations of >0.5-mg/kg body weight (b.w.) are applied.[31] Kamisaka *et al.*[31] could show, using Sephadex G-200 column chromatography, that the binding pattern of ICG to plasma proteins is concentration dependent. If a low dose ≪0.5 mg/kg b.w. is applied, ICG will be mainly bound by high molecular compartments (ß-lipoproteins, α_2-macroglobulin). A clear binding to albumin is evident only for high doses of ICG. We modified the physicochemical properties of the lipophilic indotricarbocyanine dye backbone of ICG toward a dye molecule with a low partition coefficient and low plasma protein binding, possessing a much higher hydrophilicity. As a result of these efforts, the hydrophilic dye SIDAG showed stable absorption and fluorescence properties independent of physiological environment and favorable for optical imaging.[25,29] In this study, we determined the approximate acute tolerance, evaluated the pharmacokinetic behavior and elimination characteristics of SIDAG, and performed tumor imaging experiments using a sensitive fluorescence imaging device in comparison to ICG.

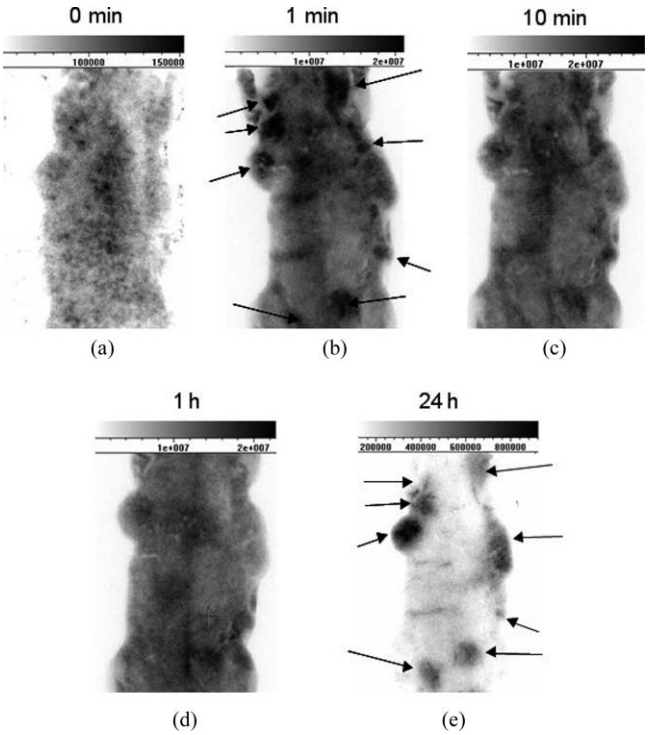

Fig. 7 Fluorescence images of tumor bearing rat (NMU-induced rat breast carcinoma) using SIDAG at a dose of 2.12 mg kg^{-1}. (a) anterior view before i.v. dye injection, (b) anterior view 1 min p.a., (c) anterior view 10 min p.a., (d) anterior view 60 min p.a., and (e) anterior view 24 h p.i. Arrows indicate tumor localization.

In order to estimate the tolerability of SIDAG, the acute tolerance was determined in a small number of animals per dose, giving a rough estimate for the approximate LD_{50}. ICG showed an approximate LD_{50} in the range of 62 mg kg^{-1}, which is close to the reported LD_{50} in mice of 60 mg kg^{-1}.[32] The hydrophilic dye SIDAG showed no signs of toxicity up to the highest dose tested of 5446 mg kg^{-1}. Assuming a diagnostic dose of 2.18 mg kg^{-1}, the dye concentration of SIDAG is 2500 times below the LD_{50} value. Compared to the margin of safety of 40 for ICG, this means a 62-fold increase in safety range using the more hydrophilic dye SIDAG. Generally, contrast media

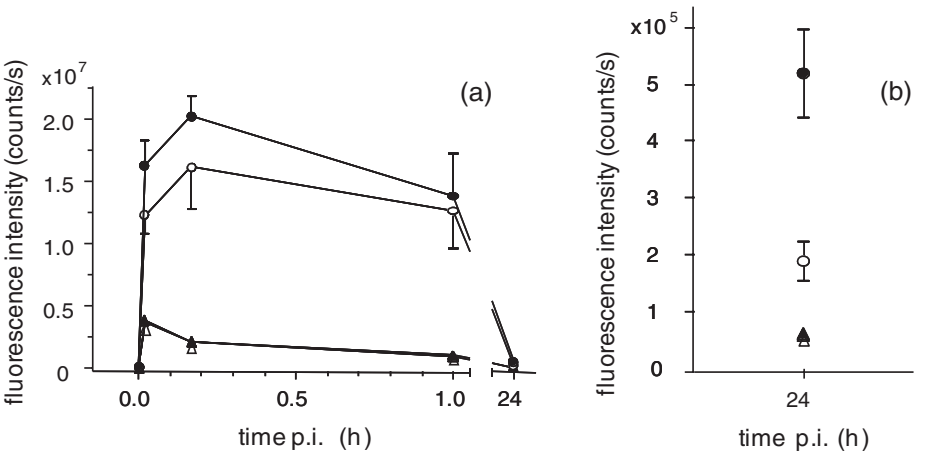

Fig. 8 Fluorescence intensities in NMU-induced rat breast tumors (filled symbols), and normal tissue (open symbols) after i.v. administration of SIDAG (●, ○) and ICG (▲, △) at a dose of 2.12 mg kg^{-1} for SIDAG and 1.55 mg kg^{-1} for ICG (a) (M ± S.D.; $n = 3$). Fluorescence intensities at 24 h p.i. at enlarged scale (b).

development with decreased plasma protein binding and lower liver uptake is often associated with an increase in tolerability. This can be explained by a considerable lower interaction of the contrast media molecule with important enzymes and receptor systems, thus possessing a more inert pharmacological profile as is highly desired for a specific diagnostic molecule.[25,26] Similar to the common contrast agents in x-ray and MRI imaging, we could also verify for the class of cyanine dyes, that extremely high doses are tolerated when the molecule exhibits comparable physicochemical properties.

The pharmacokinetic behavior of both dyes was studied in a rat model that facilitates the determination of plasma levels, renal and biliary elimination in the same animal at the same time interval. For ICG, the known profile with intravasal distribution volume, rapidly falling plasma levels, and exclusive excretion via the hepato-biliary pathway was observed. Intravasal distribution of ICG was accompanied with a high plasma clearance due to the rapid liver uptake. As a result of hydrophilic derivatization, a different pharmacokinetic profile was observed for SIDAG. The distribution of SIDAG is extravascular with distribution volumes in the range of the extracellular water. The elimination from plasma is 3.8 times slower than for ICG with a clearance of 3.2 ml min^{-1} kg^{-1}. Because SIDAG interacts with plasma proteins only to a negligible extent,[25] it is therefore accessible to glomerular filtration in the kidneys, thus shifting the elimination characteristics of the dye to renal elimination. The pharmacokinetic data of SIDAG are in the range of data known from MRI contrast media,[33,34] compounds with comparable physicochemical properties.

The distribution of fluorescence intensity of the dye SIDAG and of ICG was studied in tumors and normal tissue *in vivo* with a sensitive fluorescence imaging device. For the interpretation of fluorescence images, it is important to note that the fluorescence intensity emitted from tumors close to the surface appears much higher if compared to deeper laying tumors of the same size. However, under the same morphological conditions using comparable animal models, different contrast agents can be compared with respect to tumor enhancement as demonstrated in various studies.[7–11]

The fluorescence images of the animals in reflection geometry showed a visible but low autofluorescence in the near-infrared range. The fluorescence intensity of tumor tissue 1 min after administration of ICG or SIDAG was increased by a factor of 125 (ICG) or 197 (SIDAG) above the autofluorescence value.

During the course of imaging, larger tumors could be delineated with ICG only at 1 min p.i. according to the pharmacokinetic behavior. The quantitative image analysis showed a signal increase in tumors at 1 min after ICG administration. In accordance with the rapid liver uptake, absolute fluorescence levels fell rapidly to baseline values. Because of the faster metabolism in the rat, the time to yield sufficient enhancement in tumors for ICG-albumin complexes may not be sufficient to cope with rapid liver uptake. The highest fluorescence intensities after ICG administration were found in the liver region and, at later time points, in the gastrointestinal tract in agreement with the elimination characteristics of the dye. Nevertheless, ICG was used successfully to delineate spontaneously growing mammary tumors in canines[6,29] and in a patient study using diffuse optical mammography.[35] In the latter, the enhancement curve of ICG in the tumor region, previously localized with Gd-DTPA enhanced MRI, showed an enhancement factor of 2:1 between tumor and normal breast tissue. The fast clearance of ICG generally limits the time available during the vascular circulation for time-consuming imaging procedures. However, fast and immediate imaging investigations, such as in joint imaging[1,36] could benefit from a rapidly collapsing background. Here, kinetics has shown to provide helpful information on diseases involving disturbed microvasculature, such as inflammatory diseases.

In contrast to these findings, the low molecular hydrophilic dye SIDAG showed a much stronger signal enhancement in tumor tissue yielding a sufficient contrast for tumor delineation in the rat breast tumor model used. Because of its low plasma protein binding and its low molecular weight, SIDAG can diffuse rapidly through pores of altered tumor vessels and can thus reach deeper regions of tumor tissue in a shorter time. The enhancement factors between tumor and normal tissue are comparable to factors reported in other studies using SIDAG with 1.78 (Ref. 25) and 1.9.[26] Transferred to the situation in

human patients and in analogy to the findings using x-ray and especially MR contrast media with comparable physicochemical and pharmacokinetic profile, strong contrast enhancement could be expected. For x-ray and MR contrast media, values of 2:1 up to 10:1 were reported.[15,17] A high enhancement is of special advantage when smaller lesions in the range of the spatial resolution of diffuse optical mammography will be evaluated to increase the sensitivity of the method.

The mechanisms producing the high fluorescence contrast at 24 h p.i. using SIDAG in our rat tumor model is not known. One could speculate that this enhancement is caused by the sugar molecules used to increase the polarity of the dye molecule. The high fluorescence contrast at late time points could be confirmed in a variety of tumor xenografts of nude mice using SIDAG (data not shown) as well as in other rat mammary tumor models.[29] Furthermore, Wall *et al*. demonstrated a correlation between contrast and vascular endothelial growth factor (VEGF) expression levels.[29] These findings imply a certain molecular specificity not yet elucidated on a structural level. Analysis with near-infrared (NIR) fluorescence microscopy of freeze sections of tumor tissue showed NIR fluorescence in connective tissue and necrotic areas of tumors rather in areas of vital tumor cells.[37] The observed late (24 h) tumor contrast is mainly based on the decrease of the general dye background in the animal and a small deposited portion of dye in the tumor region. Nevertheless more dye concentration dependent studies are necessary to reveal the underlying mechanism for the late contrast enhancement.

Quantification of dye concentration in diffuse optical mammography was demonstrated by Ntziachristos *et al*.[35] and Hagen *et al*.[2] thus leading the way to follow time-dependent fluorescence enhancement of cyanine dyes in tumors. The time-dependent fluorescence enhancement of tumor tissue can be used for characterization of a lesion and thereby use optical imaging as a surrogate,[29] a method already successfully applied in contrast-enhanced MR mammography.[18,19]

In conclusion, the use of low doses of low molecular weight dyes with a favorable pharmacologic profile in combination with quantitative diffuse optical imaging seems to be a feasible approach to increase the diagnostic potential of this technique. The thorough pharmacological and toxicological characterization of dyes of simple structure beyond its sole performance in imaging models might provide a key step toward further developments for clinical application, which is challenging when the chemical and metabolic fate and long-term safety of the probe remains unclear and difficult to assess in the details required today.

Acknowledgments

We thank Anke Raddatz and Stefan Wisniewski for excellent technical assistance.

References

1. T. Fischer, B. Ebert, and J. Voigt, "Detection of rheumatoid arthritis using non-specific contrast enhanced fluorescence imaging," *Acad. Radiol.* **17**(3), 375–381 (2010).
2. A. Hagen, D. Grosenick, R. Macdonald, H. Rinneberg, S. Burock, A. Warnick, A. Poellinger, and P. M. Schlag, "Late-fluorescence mammography assesses tumor capillary permeability and differentiates malignant from benign lesions," *Opt. Express* **17**, 17016–17033 (2009).
3. V. Ntziachristos, J. S. Yoo, and G. M. van Dam, "Current concepts and future perspectives on surgical optical imaging in cancer," *J. Biomed. Opt.* **15**(6), 066024 (2010).
4. J. Boulnois, "Photo-physical processes in recent medical laser developments, a review," *Laser Med. Sci.* **1**, 47–66 (1986).
5. X. Li, B. Beauvoit, R. White, S. Nioka, B. Chance, and A. G. Yodh, "Tumor localization using fluorescence of indocyanine green (ICG) in rat models," *Proc. SPIE* **2389**, 789–798 (1995).
6. J. S. Reynolds, T. L. Troy, R. H. Mayer, A. B. Thompson, D. J. Waters, K. K. Cornell, P. W. Snyder, and E. M. Sevick-Muraca, "Imaging of spontaneous canine mammary tumors using fluorescent contrast agents," *Photochem. Photobiol.* **70**, 87–94 (1999).
7. B. Ballou, G. W. Fisher, A. S. Waggoner, D. L. Farkas, J. M. Reiland, R. Jaffe, R. B. Mujumdar, S. R. Mujumdar, and T. R. Hakala, "Tumor labeling in vivo using cyanine-conjugated monoclonal antibodies," *Cancer Immunol. Immunother.* **41**, 257–263 (1995).
8. S. Foli, P. Westermann, D. Braichotte, A. Pèlegrin, G. Wagnières, H. Van Den Bergh, and J.-P. Mach, "Antibody-indocyanin conjugates for immunophotodetection of human squamous cell carcinoma in nude mice," *Cancer Res.* **54**, 2643–2649 (1994).
9. D. Neri, B. Carnemolla, A. Nissim, A. Leprini, G. Querze, E. Balza, A. Pini, L. Tarli, C. Halin, P. Neri, L. Zardi, and G. Winter, "Targeting by affinity-matured recombinant antibody fragments of an angiogenesis associated fibronectin isoform," *Nat. Biotechnol.* **15**, 1271–1275 (1997).
10. A. Becker, B. Riefke, B. Ebert, U. Sukowski, H. Rinneberg, W. Semmler, and K. Licha, "Macromolecular contrast agents for optical imaging of tumors: Comparison of indotricarbocyanine-labeled human serum albumin and transferrin," *Photochem. Photobiol.* **71**(2), 234–241 (2000).
11. S. A. Hilderbrand and R. Weissleder, "Near-infrared fluorescence: application to *in vivo* molecular imaging," *Curr. Opin. Chem. Biol.* **14**(1), 71–79 (2010).
12. R. K. Jain, "Transport of molecules in the tumor interstitium: a review," *Cancer Res.* **47**, 3039–3051 (1987).
13. R. K. Jain, "Transport of molecules across tumor vasculature," *Cancer Metastasis Rev.* **6**, 559–593 (1987).
14. J. J. Gisvold, P. R. Karsell, and E. C. Reese, "Clinical evaluation of computerized tomographic mammography," *Mayo Clin. Proc.* **52**, 181–185 (1977).
15. A. Teifke, F. Schweden, H. Cagil, H. U. Kauczor, W. Mohr, and M. Thelen, "Spiral computerized tomography of the breast," *Rofo.* **161**, 495–500 (1994).
16. S. H. Heywang, A. Wolf, E. Pruss, T. Hilbertz, W. Eiermann, and W. Permanetta, "MR imaging of the breast with Gd-DTPA: use and limitations," *Radiology* **171**, 95–103 (1989).
17. M. Dietzel, P. A. Baltzer, T. Vag, T. Gröschel, M. Gajda, O. Camara, and W. A. Kaiser, "Magnetic resonance mammography of invasive lobular versus ductal carcinoma: systematic comparison of 811 patients reveals high diagnostic accuracy irrespective of typing," *J. Comput. Assist. Tomogr.* **34**(4), 587–597 (2010).
18. B. L. Daniel, Y. F. Yen, G. H. Glover, D. M. Ikeda, R. L. Birdwell, A. M. Sawyer-Glover, J. W. Black, S. K. Plevritis, S. S. Jeffrey, and R. J. Herfkens, "Breast disease: dynamic spiral MR imaging," *Radiology* **209**, 499–509 (1998).
19. T. H. Helbich, "Contrast enhanced magnetic resonance imaging of the breast," *Eur. J. Radiol.* **34**, 208–219 (2000).
20. A. May, S. L. Shepheard, M. Knorr, R. Effert, A. Wessing, R. J. Hargreaves, P. J. Goadsby, and H. C. Diener, "Retinal plasma extravasation in animals but not in humans: implications for the pathophysiology of migraine," *Brain* **121**, 1231–1237 (1998).
21. G. Paumgartner, P. Probst, R. Kraines, and C. M. Leevy, "Kinetics of indocyanine green removal from the blood," *NY Acad. Sci.* **170**, 134–147 (1970).
22. D. K. F. Meijer, B. Weert, and G. A. Vermeer, "Pharmacokinetics of biliary excretion in man. VI. indocyanine green," *Eur. J. Clin. Pharmacol.* **35**, 295–303 (1988).
23. W. Krause, H. Miklautz, U. Kollenkirchen, and G. Heimann, "Physicochemical parameters of X-ray contrast media," *Invest. Radiol.* **29**(1), 72–80 (1994).
24. F. Shellock and G. Kanal, "Safety of magnetic resonance imaging contrast agents," *J. Magn. Reson. Imaging* **19**, 477–487 (1999).
25. K. Licha, B. Riefke, V. Ntziachristos, A. Becker, B. Chance, and W. Semmler, "Hydrophilic cyanine dyes as contrast agents for near-infrared

tumor imaging: synthesis, photophysical properties and spectroscopic *in vivo* characterization," *Photochem. Photobiol.* **72**(3), 392–398 (2000).
26. C. Perlitz, K. Licha, F. D. Scholle, B. Ebert, M. Bahner, P. Hauff, K. T. Moesta, and M. Schirner, "Comparison of two tricarbocyanine-based dyes for fluorescence optical imaging," *J Fluoresc*. **15**(3), 443–54 (2005).
27. B. Ebert, U. Sukowski, D. Grosenick, H. Wabnitz, K. T. Moesta, K. Licha, A. Becker, W. Semmler, P. M. Schlag, and H. Rinneberg, "Near-infrared fluorescent dyes for enhanced contrast in optical mammography: phantom experiments," *J. Biomed. Opt.* **6**(2), 134–140 (2001).
28. M. Sovak, "Radiocontrast agents," *Handbook of Experimental Pharmacology*, Vol. 73, Springer-Verlag, Berlin (1984).
29. A. Wall, T. Persigehl, P. Hauff, K. Licha, M. Schirner, S. Müller, A. von Wallbrunn, L. Matuzcewski, W. Heindel, and C. Bremer, "Differentiation of angiogenic burden in human cancer xenografts using a perfusion type optical contrast agent (SIDAG)," *Breast Canc. Res.* **10**, R23 (2008).
30. R. Sharma, W. Wang, J. C. Rasmussen, A. Joshi, J. P. Houston, K. E. Adams, A. Cameron, S. Ke, S. Kwon, M. E. Mawad, and E. M. Sevick-Muraca, "Quantitative imaging of lymph function," *Am. J. Physiol. Heart Circ. Physiol.* **292**(6) H3109–H3118 (2007).
31. K. Kamisaka, Y. Yatsuji, H. Yamada, and H. Kameda, "The binding of indocyanine green and other organic anions to serum proteins in liver diseases," *Clin. Chim. Acta* **53**, 255–264 (1974).
32. U. Speck, "Contrast media—overview, use and pharmaceutical aspects," 4th rev. version, Springer-Verlag, Berlin (1999).
33. H. Vogler, J. Platzek, G. Schuhmann-Giampieri, T. Frenzel, H. J. Weinmann, B. Radüchel, and W. R. Press, "Pre-clinical evaluation of gadobutrol: a new, neutral, extracellular contrast agent for magnetic resonance imaging," *Eur. J. Radiol.* **21**(1), 1–10 (1995).
34. H. J. Weinmann, "Characteristics of Gd-DTPA dimeglumine," in *Magnevist Monograph*, 3th ed., R. Felix, A. Heshiki, N. Hosten, H. Hricak, Eds., pp. 5–14, Blackwell Science, Berlin (1998).
35. V. Ntziachristos, A. G. Yodh, M. Schnall, and B. Chance, "Concurrent MRI and diffuse optical tomography of breast following indocyanine green enhancement," *Proc. Nat. Acad. Sci. U S A* **97**, 2767–2772 (2000).
36. T. Fischer, I. Gemeinhardt, S. Wagner, D. V. Stieglitz, J. Schnorr, K. G. Hermann, B. Ebert, D. Petzelt, R. Macdonald, K. Licha, M. Schirner, V. Krenn, T. Kamradt, and M. Taupitz, "Assessment of unspecific near-infrared dyes in laser-induced fluorescence imaging of experimental arthritis," *Acad. Radiol.* **13**(1), 4–13 (2006).
37. B. Riefke and A. Becker, unpublished data (2001).